REPORT

NEUROSCIENCE

The paraventricular thalamus is a critical thalamic area for wakefulness

Shuancheng Ren[1]*, Yaling Wang[1]*, Faguo Yue[1,2]*, Xiaofang Cheng[1], Ruozhi Dang[1], Qicheng Qiao[1], Xueqi Sun[1], Xin Li[1], Qian Jiang[2], Jiwei Yao[3], Han Qin[3], Guanzhong Wang[1], Xiang Liao[3], Dong Gao[2], Jianxia Xia[1], Jun Zhang[1], Bo Hu[1], Junan Yan[3], Yanjiang Wang[4], Min Xu[5], Yunyun Han[6], Xiangdong Tang[7], Xiaowei Chen[3]†, Chao He[1]†, Zhian Hu[1]†

Clinical observations indicate that the paramedian region of the thalamus is a critical node for controlling wakefulness. However, the specific nucleus and neural circuitry for this function remain unknown. Using in vivo fiber photometry or multichannel electrophysiological recordings in mice, we found that glutamatergic neurons of the paraventricular thalamus (PVT) exhibited high activities during wakefulness. Suppression of PVT neuronal activity caused a reduction in wakefulness, whereas activation of PVT neurons induced a transition from sleep to wakefulness and an acceleration of emergence from general anesthesia. Moreover, our findings indicate that the PVT–nucleus accumbens projections and hypocretin neurons in the lateral hypothalamus to PVT glutamatergic neurons' projections are the effector pathways for wakefulness control. These results demonstrate that the PVT is a key wakefulness-controlling nucleus in the thalamus.

Patients with occlusion of the paramedian thalamic artery, which results in localized injury to the paramedian region of the thalamus, show disturbances of consciousness ranging from hypersomnolence to sleep-like coma when injuries are bilateral (*1*–*4*), a clinical feature not observed in other thalamic injuries (*2*). The homologous area of the primate paramedian thalamus in rodents consists of a large number of nuclei, including the paraventricular thalamus (PVT), nucleus reuniens, mediodorsal nucleus, and interanteromedial thalamic nucleus (*5*, *6*). These nuclei have distinct input and output connections (*6*–*8*) and participate in various brain functions (*5*, *9*, *10*). However, the specific nucleus and circuitry controlling wakefulness have not yet been identified.

We began by visualizing an unbiased map of c-fos expression in the paramedian thalamus after a period of wakefulness or sleep in mice. We observed a higher level of c-fos expression in the PVT than in the other nuclei of the paramedian thalamus at zeitgeber time 18 (ZT 18; 24:00) and after extended wakefulness (fig. S1). To further examine the in vivo dynamics of PVT neurons during the sleep-wake cycle, we injected adeno-associated virus (AAV) expressing the genetically encoded Ca^{2+} sensor GCaMP6f under the control of the CaMKIIα promoter (PVT neurons are primarily glutamatergic neurons) (*11*) into the PVT (fig. S2, A and B). The population Ca^{2+} activity was significantly higher during wakefulness than during sleep. The population Ca^{2+} activity of the PVT began to increase ahead of signs of behavioral arousal (fig. S2, C to H). We next performed in vivo multichannel electrophysiological recordings to monitor the spike firing of individual PVT neurons in freely behaving mice (Fig. 1A). The vast majority (20/22) of PVT neurons exhibited a higher firing rate during wakefulness than during sleep (Fig. 1, B and C). The PVT firing rate gradually decreased before sleep onset and increased during transitions from sleep to wakefulness. At the onset of behavioral arousal from non–rapid eye movement (NREM) sleep, the mean firing rate reached 7.1 Hz (Fig. 1, D to F). In a considerable fraction of neurons (25%), the firing rate exceeded 10 Hz (fig. S3). The increase of PVT neuronal firing occurred briefly before both cortical activation (1.0 ± 0.3 s) and behavioral arousal (1.4 ± 0.3 s).

We next determined the necessity of PVT activity for wakefulness by inhibiting PVT glutamatergic neurons chemogenetically with AAV encoding engineered G_i-coupled hM4D receptor (AAV-CaMKIIα-hM4D-mCherry) (Fig. 1G). Whole-cell recordings of PVT neurons from acute brain slices confirmed that clozapine-*N*-oxide (CNO, 5 μM) potently inhibited hM4D-expressing PVT neurons (fig. S4). At the beginning of the dark phase (ZT 12; 18:00), CNO injection induced a significant reduction in wakefulness relative to the mCherry and saline controls (Fig. 1, H and I, and fig. S6A), which was primarily due to shortened duration of wakefulness episodes and increased sleep episodes (fig. S5). In addition, spectral analysis of electroencephalography (EEG) showed that CNO injection increased the high delta power (2 to 4 Hz) of wakefulness at hour 2 after CNO injection (figs. S6 and S7). Note that inhibition of the PVT increased the number of micro-arousals (fig. S8, A and B), which might result from a fragmentation of wakefulness. In contrast, CNO injection at the beginning of the light phase (ZT 0; 6:00) did not further reduce wakefulness (fig. S9, A, D, and G). The EEG power spectrum for each state and the number of micro-arousals during the light phase were not affected by CNO injection (figs. S8C and S9).

We next explored the role of the PVT in controlling wakefulness by ablating PVT glutamatergic neurons. We injected a mixture of AAV encoding diphtheria toxin A (AAV-DIO-DTA) and AAV-CaMKIIα-Cre-GFP into the PVT. PVT glutamatergic neurons were selectively ablated after 4 weeks of virus injection (fig. S10A). Animals with chronic PVT lesion showed a decrease of wakefulness during the dark phase, with a reduction in duration of wakefulness episodes and an increase in NREM sleep episodes and micro-arousals, whereas lesion of the PVT did not affect wakefulness during the light phase (fig. S10, B to G). DTA lesion increased the EEG high delta power (2 to 4 Hz) of wakefulness during the dark phase. This lesion also caused an increase in the low theta power (4 to 7 Hz) (fig. S10, H to L), which might reflect a compensatory mechanism during chronic ablation of neurons induced by DTA. In addition, we also injected ibotenic acid to rapidly ablate PVT neurons within several days (Fig. 1J and fig. S11A). Acute PVT lesion reduced wakefulness during the dark phase but did not affect wakefulness during the light phase (Fig. 1K and fig. S11, B and C). Lesion of the PVT caused fragmentation of wakefulness, which was indicated by shortened duration of wakefulness episodes and by increased sleep bouts and micro-arousals during the dark phase. In contrast to chronic lesion, ibotenic acid lesion increased the EEG high delta power (2 to 4 Hz) but not the theta power, indicating a more typical damage to the wakefulness state (Fig. 1L, fig. S11, D to J, and movie S1).

We then used optogenetics to examine the causal role of the PVT in wakefulness control. We injected AAV expressing channelrhodopsin 2 (AAV-CaMKIIα-ChR2-mCherry) into the PVT (Fig. 2A). Functional expression of ChR2 was verified by in vitro electrophysiology (Fig. 2B). We applied optical stimulation (lasting 20 s) after the onset of stable NREM or REM sleep during the light phase. Optical stimulation of PVT glutamatergic neurons during NREM sleep

[1]Department of Physiology, Collaborative Innovation Center for Brain Science, Third Military Medical University, Chongqing 400038, China. [2]Department of Sleep and Psychology, Daping Hospital, Third Military Medical University, Chongqing 400042, China. [3]Brain Research Center, Third Military Medical University, Chongqing 400038, China. [4]Department of Neurology, Daping Hospital, Third Military Medical University, Chongqing 400042, China. [5]Institute of Neuroscience, State Key Laboratory of Neuroscience, Shanghai Institutes for Biological Sciences, Chinese Academy of Sciences, Shanghai 200031, China. [6]Department of Neurobiology, School of Basic Medicine and Tongji Medical College, Huazhong University of Science and Technology, Wuhan 430030, China. [7]Sleep Medicine Center, Laboratory of Anaesthesia and Critical Care Medicine, Translational Neuroscience Center, West China Hospital, Sichuan University, Chengdu 610041, China.
*These authors contributed equally to this work.
†Corresponding author. Email: xiaowei_chen@tmmu.edu.cn (X.C.); hechaochongqing@163.com (C.H.); zhianhu@aliyun.com (Z.H.)

reliably induced transitions to wakefulness in a frequency-dependent manner (Fig. 2, C and D). Optical stimulation of the PVT at a shorter duration (lasting 5 s) was still sufficient to induce such transitions (fig. S12). Optical stimulation also induced transitions to wakefulness from REM sleep (fig. S13, A and B). Optical stimulation significantly increased the probability of wakefulness, along with a complementary decrease of both NREM and REM sleep probability, relative to the mCherry control (Fig. 2E and fig. S13, C and D). We also delivered prolonged optical stimulation to test the ability of PVT neurons in maintaining wakefulness (fig. S14A). Such optical stimulation resulted in an

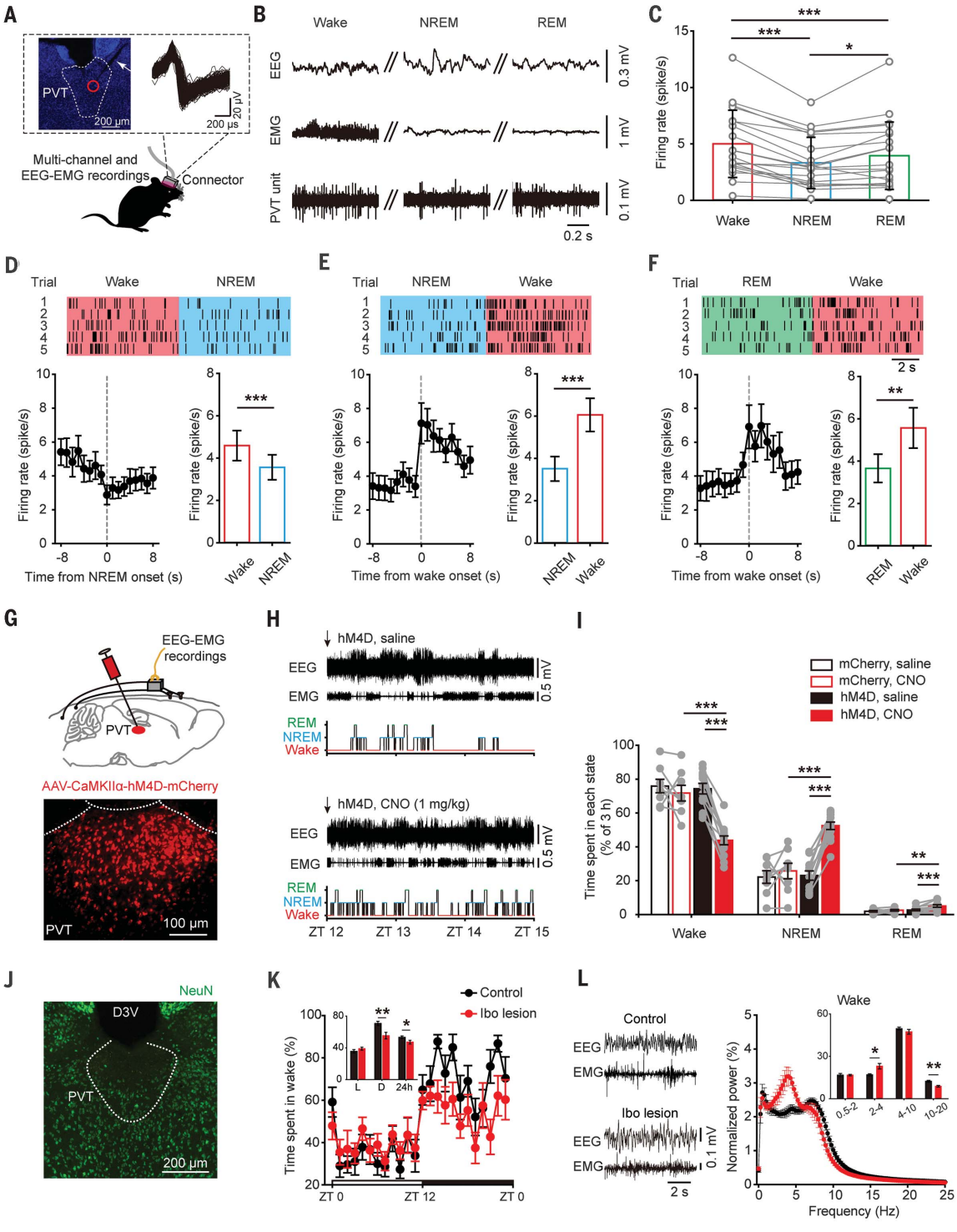

Fig. 1. PVT glutamatergic neurons are required for the control of wakefulness. (**A**) Schematic configuration of in vivo multichannel electrophysiological recordings. Left inset: A brain slice from a mouse with electrodes implanted in the PVT. White arrow indicates the electrode track. Red circle indicates the recording position. Right inset: Waveforms from a recorded PVT neuron. (**B**) EEG, electromyography (EMG), and PVT unit recording traces during wakefulness, NREM sleep, and REM sleep. (**C**) Average firing rate of PVT neurons in each state. (**D** to **F**) Firing rate of PVT neurons during state transitions: wake-to-NREM (D), NREM-to-wake (E), and REM-to-wake (F). Top: Example rastergrams of a PVT neuron during five trials of different state transitions. Bottom left: Average firing rate during the state transition period. Bottom right: Average firing rate of 8 s before and after state transitions. (**G**) Top: Schematic of virus injection and EEG-EMG recordings. Bottom: Image showing the expression of hM4D-mCherry in PVT neurons. (**H**) EEG-EMG traces and hypnograms during 3 hours after saline or CNO (1 mg/kg) injection in an hM4D-mCherry mouse. (**I**) Percentage of time spent in each state during 3 hours after injection. (**J**) Image showing NeuN (neuron-specific nuclear protein) staining from a mouse with PVT lesion using ibotenic acid (Ibo). (**K**) Hourly percentage of time spent in wakefulness across the 24-hour sleep-wake cycle. L, light phase; D, dark phase. (**L**) Left: Raw EEG-EMG traces of wakefulness. Right: Normalized EEG power density of wakefulness during the dark phase. Inset in (L) is a quantitative analysis of the power in different frequency bands. *P < 0.05, **P < 0.01, ***P < 0.001. Error bars denote SEM. See table S1 for further details of statistical data analysis.

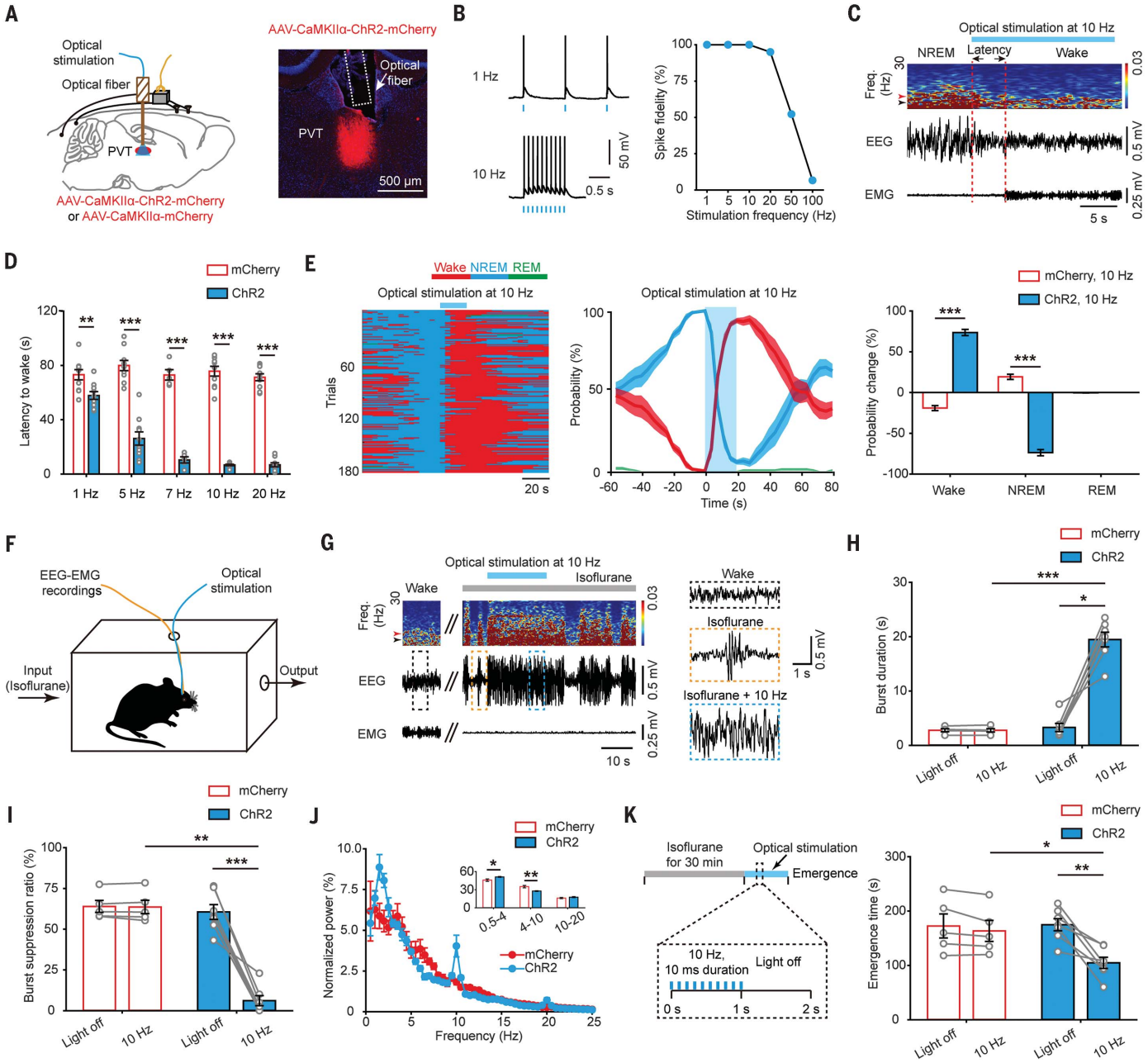

Fig. 2. Optogenetic activation of PVT glutamatergic neurons induces wakefulness from sleep and general anesthesia. (**A**) Left: Schematic of optogenetic manipulation of PVT glutamatergic neurons and EEG-EMG recordings. Right: ChR2-mCherry expression and location of optical fiber in the PVT. (**B**) Example traces (left) and fidelity of action potential firing (right) of ChR2-expressing PVT neurons evoked by 473-nm light stimulation with different frequencies. (**C**) Representative EEG power spectrum and EEG-EMG traces around 10-Hz stimulation delivered during NREM sleep. Arrowheads indicate 4 Hz and 8 Hz. Color scale indicates the power (mV^2) of raw power spectral density. Fre., frequency. (**D**) Latency to wakefulness from NREM sleep after optical activation at 1 Hz, 5 Hz, 7 Hz, 10 Hz, or 20 Hz. (**E**) Left: Brain states in all trials from ChR2-expressing mice. Center: Probability of each state around optogenetic stimulation delivered during NREM sleep. Right: Probability change of each state 20 s before and during optical stimulation. (**F**) Experimental setup for EEG-EMG recordings with simultaneous optogenetic activation in the presence of continuous isoflurane. (**G**) Left: EEG power spectrum and EEG-EMG traces around 10-Hz stimulation during isoflurane-induced general anesthesia. Right: Enlarged view of EEG activity during wakefulness, isoflurane-induced anesthesia, and 10-Hz optical stimulation in continuous isoflurane conditions. (**H** and **I**) Burst duration (H) and burst suppression ratio (I) during periods of light off and 10-Hz optical stimulation. (**J**) Spectral analysis of EEG activity during optical stimulation in the presence of isoflurane. (**K**) Left: Schematic of sustained optical stimulation protocol after the discontinuation of isoflurane. Right: Emergence time during light off and 10-Hz optical stimulation. *P < 0.05, **P < 0.01, ***P < 0.001. Error bars denote SEM. See table S1 for further details of statistical data analysis.

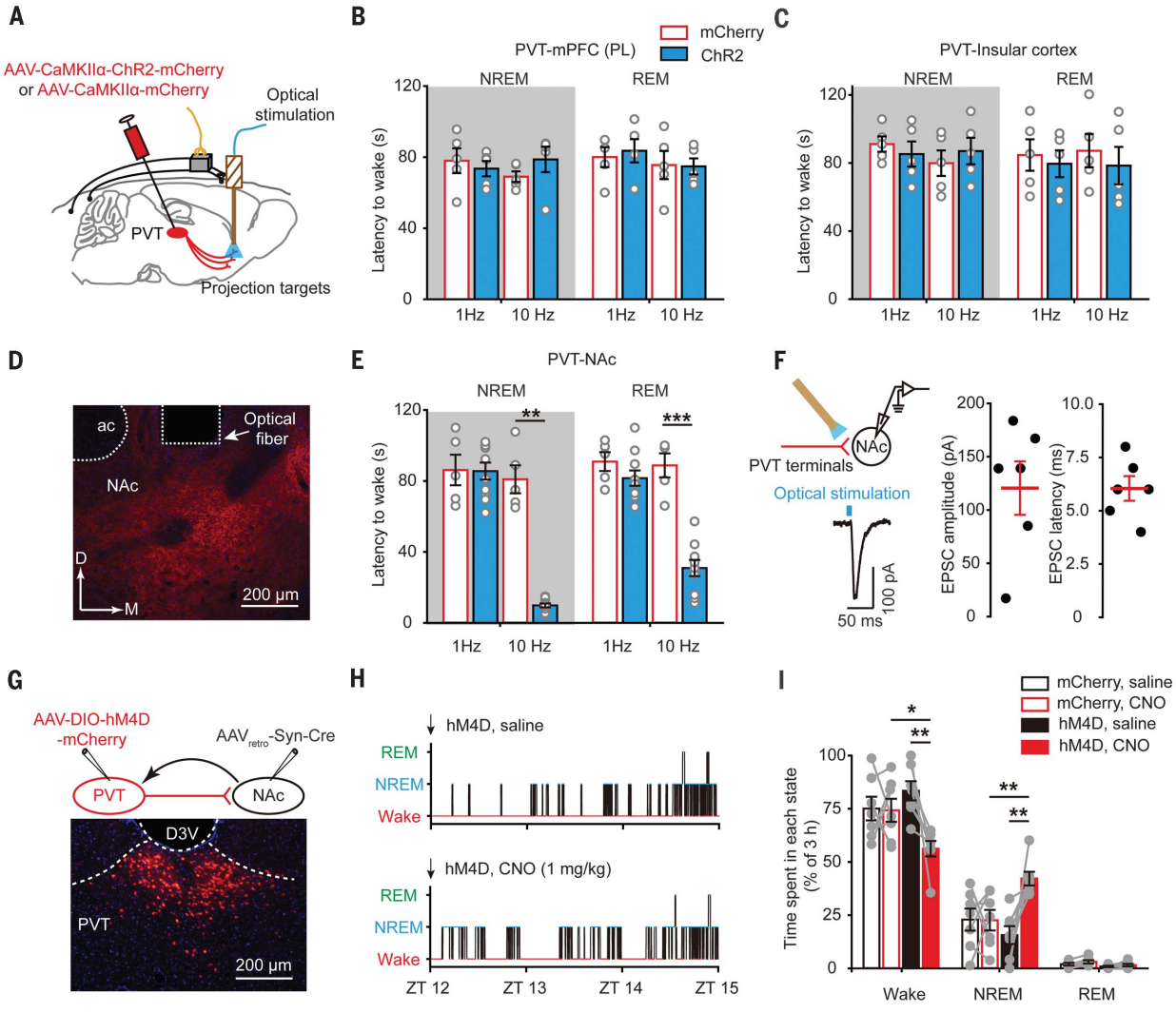

Fig. 3. PVT glutamatergic neurons control wakefulness through the PVT-NAc pathway. (**A**) Schematic of optogenetic stimulation of ChR2-expressing PVT glutamatergic terminals together with EEG-EMG recordings. (**B** and **C**) Latency to wakefulness from NREM and REM sleep after stimulation of PVT projections to the prelimbic cortex (PL) of the mPFC (B) and to the insular cortex (C) at 1 or 10 Hz. (**D**) Distribution of ChR2-expressing PVT glutamatergic terminals and location of optical fiber in the NAc. D, dorsal; M, medial; ac, anterior commissure. (**E**) Latency to wakefulness from NREM and REM sleep after activation of the PVT-NAc pathway at 1 or 10 Hz. (**F**) Top left: Experimental paradigm for in vitro characterization of functional connection of the PVT to NAc. Bottom left: Trace of the single optical stimulation–evoked excitatory postsynaptic currents (EPSCs) in NAc neurons. Right: Amplitude and latency of optical stimulation–evoked EPSCs. (**G**) Top: Experimental design of chemogenetic inhibition of the NAc-projecting PVT neurons. Bottom: Expression of hM4D-mCherry in NAc-projecting PVT neurons. D3V, dorsal third ventricle. (**H**) Hypnograms of an hM4D-mCherry mouse during 3 hours after saline or CNO injection. (**I**) Percentage of time spent in each state during 3 hours after injection. *P < 0.05, **P < 0.01, ***P < 0.001. Error bars denote SEM. See table S1 for further details of statistical data analysis.

overt increase in wakefulness with a decrease of EEG delta power (fig. S14, B to F).

To investigate whether activation of PVT neurons is sufficient to induce wakefulness from an unconscious state—a typical feature of patients with paramedian thalamic stroke (*4*)—we optically activated PVT neurons in mice under general anesthesia induced by isoflurane (Fig. 2F). When a stable EEG burst-suppression mode (a marker of anesthetic depth) (*12*) was observed, 10-Hz stimulation (lasting 20 s) caused an immediate increase in total EEG burst activity. The increase in burst activity was accompanied by a prolonged burst duration, a decreased burst suppression ratio, and an altered EEG spectrum (Fig. 2, G to J). Interestingly, a peak at approximately 10 Hz appeared in the EEG spectrum with optical stimulation (Fig. 2J), which might reflect that optogenetic stimulation at 10 Hz causes prominent 10-Hz oscillations in cortex. Additionally, sustained activation of PVT neurons significantly accelerated the emergence from isoflurane-induced unconsciousness, which was not observed in mCherry mice (Fig. 2K).

Recent studies have reported that thalamic nuclei directly regulate the activities of cortical neurons (*13*, *14*). The PVT also sends brainwide projections, including direct projections to the cortex (*15*). Thus, we next searched for the PVT downstream pathways mediating the wakefulness-maintaining effects. ChR2-mCherry expression indicated that PVT glutamatergic neurons send projections to multiple cortical regions, including the medial prefrontal cortex (mPFC) and insular cortex (fig. S15, A to D). The PVT sends dense projections to the nucleus accumbens (NAc) (Fig. 3D), which participates in wakefulness control (*16*). Bilateral optical stimulation of PVT projections to different layers or subregions of the prelimbic cortex of the mPFC failed to induce rapid transitions from NREM sleep to wakefulness. Optical stimulation of PVT axonal terminals in other cortical regions, including the cingulate cortex and infralimbic cortex of the mPFC or the anterior and posterior

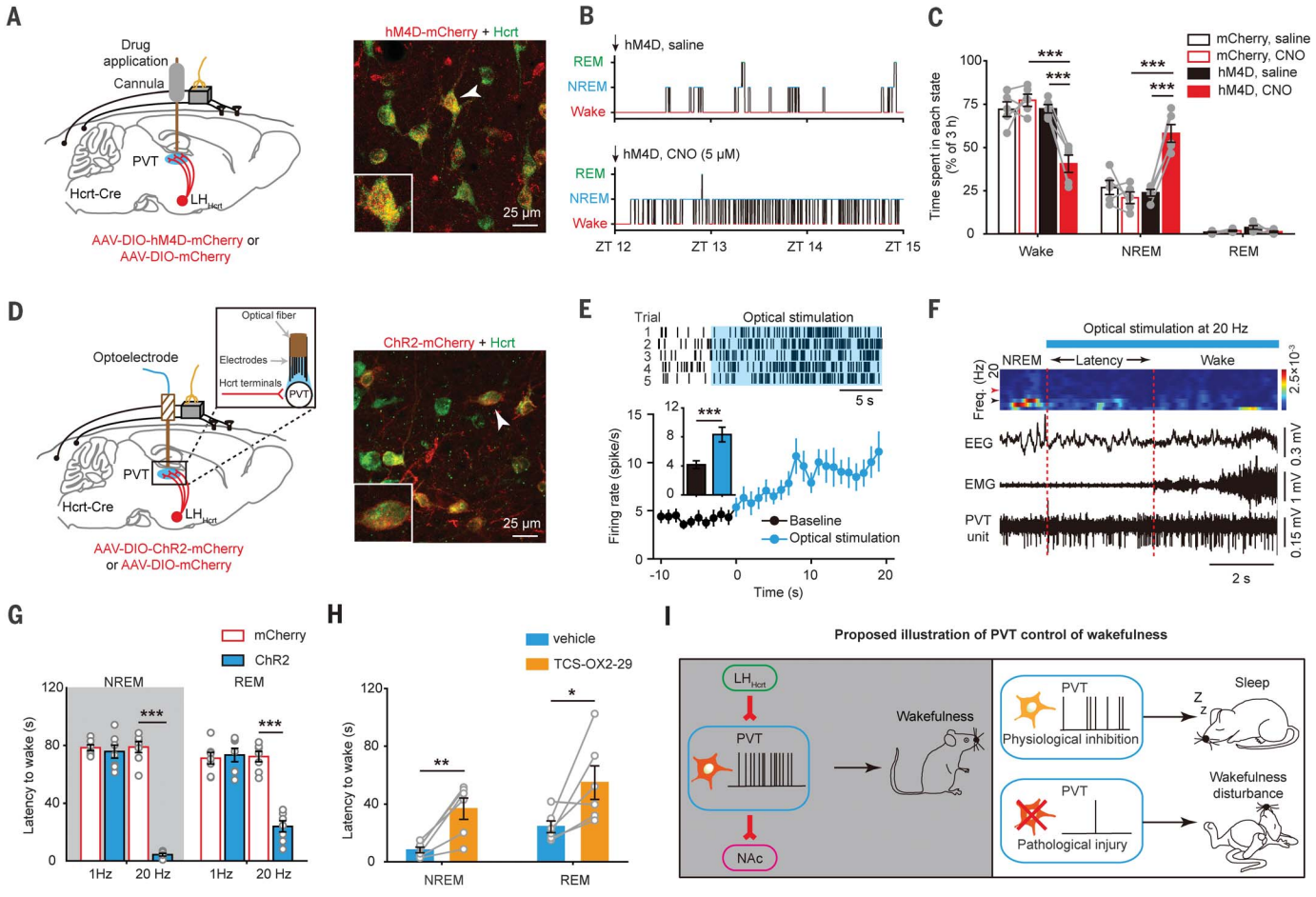

Fig. 4. The wakefulness-controlling function of the PVT is regulated by Hcrt neurons. (**A**) Left: Schematic of chemogenetic inhibition of LH_{Hcrt}-PVT pathway and EEG-EMG recordings. Right: Selective expression of hM4D-mCherry in Hcrt neurons in the LH. Arrowhead denotes neuron shown in close-up (inset). (**B**) Hypnograms of an hM4D-mCherry mouse during 3 hours after saline or CNO (5 μM) local infusion. (**C**) Percentage of time spent in each state during 3 hours after injection. (**D**) Left: Schematic of optogenetic stimulation of LH_{Hcrt}-PVT pathway together with PVT unit and EEG-EMG recordings. Right: ChR2-mCherry expression in Hcrt neurons in the LH. Arrowhead denotes neuron shown in close-up (inset). (**E**) Top: Rastergrams showing the firing activity of a PVT neuron before and during optical stimulation. Bottom: Optical stimulation of Hcrt neurons' terminals significantly increased the average firing rate of PVT neurons. (**F**) EEG-EMG traces and PVT unit firing around 20-Hz optical stimulation in a freely moving mouse. (**G**) Latency to wakefulness from NREM or REM sleep after optical stimulation at 1 or 20 Hz. (**H**) The Hcrt receptor antagonist TCS-OX2-29 attenuated the wakefulness-inducing effects of optical stimulation of Hcrt neuron's terminals in the PVT. (**I**) Model of the PVT control of wakefulness. Left: Increased levels of Hcrt may activate Hcrt inputs to the PVT, which could excite PVT neurons projecting to the NAc, thereby activating NAc neurons to control wakefulness. Top right: Decreased activity of PVT neurons leads to sleep. Bottom right: The impairment of PVT neurons seen in neurological diseases may be associated with disturbances of wakefulness. $^*P < 0.05$, $^{**}P < 0.01$, $^{***}P < 0.001$. Error bars denote SEM. See table S1 for further details of statistical data analysis.

part of the insular cortex, had no obvious effects on sleep-wake transition (Fig. 3, A to C, and fig. S15, E and F), although the paramedian thalamus can excite these cortices via glutamatergic connections (*17*). Moreover, chemogenetic inhibition of the mPFC-projecting PVT neurons also did not affect the time spent in wakefulness (fig. S16). Together, our results do not sufficiently support a crucial role of the PVT-cortex pathway in controlling wakefulness. However, optical stimulation of the PVT-to-NAc projections reliably elicited transitions to wakefulness from both NREM and REM sleep (Fig. 3E). In vitro ChR2-assisted circuit mapping (*18*) confirmed this functional monosynaptic connection (Fig. 3F), indicating that a direct PVT-NAc pathway may mediate the observed transitions. In addition, chemogenetic inhibition of NAc-projecting PVT neurons significantly reduced wakefulness (Fig. 3, G to I). The importance of this pathway in wakefulness control was further confirmed by the compromised wakefulness-inducing effects of the PVT after ablation of NAc neurons using ibotenic acid (fig. S17). Manipulation of the PVT-NAc pathway efficiently reproduced the wakefulness-controlling effects of the PVT (fig. S18).

Because the PVT receives inputs from the brainstem and lateral hypothalamus (LH) (*19*, *20*), we next searched for the upstream pathway that modulates its wakefulness-maintaining function. We used Cre-dependent rabies virus–mediated monosynaptic retrograde tracing in vGlut2-Cre mice and found that PVT glutamatergic neurons received direct inputs from LH hypocretin (Hcrt) neurons (fig. S19), which are involved in wakefulness control (*21*). We specifically suppressed inputs from Hcrt neurons by expressing AAV-DIO-hM4D-mCherry in the LH of Hcrt-Cre mice and locally applying CNO (5 μM) in the PVT (Fig. 4A). CNO infusion significantly decreased wakefulness, accompanied by fragmentation of wakefulness (Fig. 4, B and C, and fig. S20, A to D). Moreover, inhibition of this pathway shortened NREM sleep latency and increased the number of NREM sleep episodes (fig. S20, E and F).

We then examined the sufficiency of these inputs for wakefulness control. Optical stimulation (20 Hz) of Hcrt neurons' terminals during NREM sleep significantly increased the firing rate of PVT neurons (Fig. 4, D and E). At the behavioral level, apparent transitions from sleep

to wakefulness occurred after stimulation of the LH_{Hcrt}-PVT pathway (Fig. 4, F and G, and fig. S21). Optogenetic stimulation of Hcrt neurons' terminals in the PVT could still induce transitions from sleep to wakefulness after blockade of the potential antidromic action potentials by injection of muscimol into the LH (fig. S22). Such wakefulness-controlling effects were partially attenuated by the Hcrt receptor 2 antagonist TCS-OX2-29 (Fig. 4H). To further confirm the importance of the LH_{Hcrt}-PVT pathway in controlling wakefulness, we injected viruses expressing hM3D into the LH and hM4D into the PVT, respectively (fig. S23, A and B). Stimulation of Hcrt neurons increased the amount of wakefulness, whether or not the PVT was chemogenetically inhibited (fig. S23C). These unexpected results might be because the activity of the PVT was not completely suppressed under the condition of activating Hcrt neurons' terminals. Alternatively, after ablating PVT neurons using caspase-3, the latency to wakefulness with optogenetic stimulation of Hcrt neurons increased, confirming an important role of the LH_{Hcrt}-PVT pathway in wakefulness control (fig. S23, D to G).

Recently, the PVT in the paramedian thalamus has been extensively studied because of its involvement in multiple behaviors, including fear conditioning (*22*, *23*), drug addiction (*24*, *25*), and feeding (*26*), all of which require elevated wakefulness. Our results demonstrate that the PVT is both necessary and sufficient for the control of wakefulness, and further reveal the important role of the LH_{Hcrt}-PVT-NAc pathway in the control of wakefulness (Fig. 4I). These results provide experimental evidence supporting the PVT as a critical thalamic node in the wakefulness-controlling neural network.

REFERENCES AND NOTES

1. G. Percheron, *Z. Neurol.* **205**, 1–13 (1973).
2. J. D. Schmahmann, *Stroke* **34**, 2264–2278 (2003).
3. A. Honig *et al*., *J. Clin. Neurosci.* **34**, 81–85 (2016).
4. D. M. Hermann *et al*., *Stroke* **39**, 62–68 (2008).
5. R. P. Vertes, S. B. Linley, W. B. Hoover, *Neurosci. Biobehav. Rev.* **54**, 89–107 (2015).
6. H. J. Groenewegen, H. W. Berendse, *Trends Neurosci.* **17**, 52–57 (1994).
7. H. Jasper, *Electroencephalogr. Clin. Neurophysiol.* **1**, 405–419 (1949).
8. K. E. Krout, R. E. Belzer, A. D. Loewy, *J. Comp. Neurol.* **448**, 53–101 (2002).
9. W. Xu, T. C. Südhof, *Science* **339**, 1290–1295 (2013).
10. Y. D. Van der Werf, M. P. Witter, H. J. Groenewegen, *Brain Res. Rev.* **39**, 107–140 (2002).
11. C. Frassoni, R. Spreafico, M. Bentivoglio, *Exp. Brain Res.* **115**, 95–104 (1997).
12. P. C. Vijn, J. R. Sneyd, *Br. J. Anaesth.* **81**, 415–421 (1998).
13. S. Honjoh *et al*., *Nat. Commun.* **9**, 2100 (2018).
14. T. C. Gent, M. Bandarabadi, C. G. Herrera, A. R. Adamantidis, *Nat. Neurosci.* **21**, 974–984 (2018).
15. R. P. Vertes, W. B. Hoover, *J. Comp. Neurol.* **508**, 212–237 (2008).
16. Y. J. Luo *et al*., *Nat. Commun.* **9**, 1576 (2018).
17. P. M. Fogerson, J. R. Huguenard, *Neuron* **92**, 687–704 (2016).
18. L. Petreanu, D. Huber, A. Sobczyk, K. Svoboda, *Nat. Neurosci.* **10**, 663–668 (2007).
19. S. Li, G. J. Kirouac, *Brain Struct. Funct.* **217**, 257–273 (2012).
20. G. J. Kirouac, M. P. Parsons, S. Li, *Brain Res.* **1059**, 179–188 (2005).
21. J. Li, Z. Hu, L. de Lecea, *Br. J. Pharmacol.* **171**, 332–350 (2014).
22. M. A. Penzo *et al*., *Nature* **519**, 455–459 (2015).
23. F. H. Do-Monte, K. Quiñones-Laracuente, G. J. Quirk, *Nature* **519**, 460–463 (2015).
24. Y. Zhu, C. F. Wienecke, G. Nachtrab, X. Chen, *Nature* **530**, 219–222 (2016).
25. G. J. Kirouac, *Neurosci. Biobehav. Rev.* **56**, 315–329 (2015).
26. X. Zhang, A. N. van den Pol, *Science* **356**, 853–859 (2017).

ACKNOWLEDGMENTS

We thank L. de Lecea for providing the Hcrt-Cre mice, and M. M. Luo and Y. M. Lu for critical comments on the manuscript. **Funding:** Supported by the National Natural Science Foundation of China (31771192 to Z.H., 31500862 to C.H., and 81671106 to X.W.C.) and "973 Program" (2015CB759500 to X.W.C.). **Author contributions:** S.R., C.H., and Z.H. designed the study; S.R., Y.L.W., F.Y., X.F.C., R.D., Q.Q., H.Q., J.W.Y., J.A.Y., G.W., X. Li, Y.J.W., and C.H. executed the experiments and performed statistical analysis; Q.J., X.S., X. Liao, D.G., J.X., J.Z., B.H., X.T., and X.W.C. analyzed the data; S.R., C.H., and Z.H. wrote the paper with the help of Y.J.W., M.X., Y.H., X.T., and X.W.C.; and all authors read and commented on the manuscript. Z.H. supervised all aspects of the project. **Competing interests:** The authors declare no competing interests. **Data and materials availability:** All data necessary to understand and assess the conclusions of this manuscript are available in the paper and the supplementary materials.

SUPPLEMENTARY MATERIALS

www.sciencemag.org/content/362/6413/429/suppl/DC1
Materials and Methods
Figs. S1 to S25
Table S1
References (*27*–*40*)
Movie S1

8 March 2018; accepted 6 September 2018
10.1126/science.aat2512

The paraventricular thalamus is a critical thalamic area for wakefulness

Shuancheng Ren, Yaling Wang, Faguo Yue, Xiaofang Cheng, Ruozhi Dang, Qicheng Qiao, Xueqi Sun, Xin Li, Qian Jiang, Jiwei Yao, Han Qin, Guanzhong Wang, Xiang Liao, Dong Gao, Jianxia Xia, Jun Zhang, Bo Hu, Junan Yan, Yanjiang Wang, Min Xu, Yunyun Han, Xiangdong Tang, Xiaowei Chen, Chao He and Zhian Hu

Science **362** (6413), 429-434.
DOI: 10.1126/science.aat2512

A close view of the paraventricular thalamus

The paraventricular thalamus is a relay station connecting brainstem and hypothalamic signals that represent internal states with the limbic forebrain that performs associative functions in emotional contexts. Zhu *et al.* found that paraventricular thalamic neurons represent multiple salient features of sensory stimuli, including reward, aversiveness, novelty, and surprise. The nucleus thus provides context-dependent salience encoding. The thalamus gates sensory information and contributes to the sleep-wake cycle through its interactions with the cerebral cortex. Ren *et al.* recorded from neurons in the paraventricular thalamus and observed that both population and single-neuron activity were tightly coupled with wakefulness.

Science, this issue p. 423, p. 429